Effects of electrode material and configuration on the characteristics of planar resistive switching devices

H. Y. Peng, L. Pu, J. C. Wu, D. Cha, J. H. Hong, W. N. Lin, Y. Y. Li, J. F. Ding, A. David, K. Li, and T. Wu

Citation: APL Materials **1**, 052106 (2013); doi: 10.1063/1.4827597
View online: http://dx.doi.org/10.1063/1.4827597
View Table of Contents: http://scitation.aip.org/content/aip/journal/aplmater/1/5?ver=pdfcov
Published by the AIP Publishing

APL MATERIALS **1**, 052106 (2013)

Effects of electrode material and configuration on the characteristics of planar resistive switching devices

H. Y. Peng,[1,2] L. Pu,[1] J. C. Wu,[3] D. Cha,[4] J. H. Hong,[4] W. N. Lin,[1] Y. Y. Li,[5] J. F. Ding,[5] A. David,[1] K. Li,[4] and T. Wu[5,a]

[1]*Division of Physics and Applied Physics, School of Physical and Mathematical Sciences, Nanyang Technological University, 21 Nanyang Link, Singapore 637371, Singapore*
[2]*Advanced LSI Technology Laboratory, Corporate Research and Development Center, Toshiba Corporation, Kawasaki 212-8582, Japan*
[3]*Key Laboratory of Radiation Physics and Technology, Ministry of Education, Institute of Nuclear Science and Technology, Sichuan University, Chengdu 610064, China*
[4]*Imaging and Characterization Core Lab, King Abdullah University of Science and Technology, Thuwal 23955, Saudi Arabia*
[5]*Materials Sciences and Engineering, King Abdullah University of Science and Technology, Thuwal 23955, Saudi Arabia*

(Received 19 June 2013; accepted 14 October 2013; published online 13 November 2013)

We report that electrode engineering, particularly tailoring the metal work function, measurement configuration and geometric shape, has significant effects on the bipolar resistive switching (RS) in lateral memory devices based on self-doped $SrTiO_3$ (STO) single crystals. Metals with different work functions (Ti and Pt) and their combinations are used to control the junction transport (either ohmic or Schottky-like). We find that the electric bias is effective in manipulating the concentration of oxygen vacancies at the metal/STO interface, influencing the RS characteristics. Furthermore, we show that the geometric shapes of electrodes (e.g., rectangular, circular, or triangular) affect the electric field distribution at the metal/oxide interface, thus plays an important role in RS. These systematic results suggest that electrode engineering should be deemed as a powerful approach toward controlling and improving the characteristics of RS memories. [http://dx.doi.org/10.1063/1.4827597]

Electric-field-induced resistive switching (RS) has attracted lots of attention due to the promising applications in resistive random access memory (RRAM).[1–12] RS devices have various prominent advantages like good scalability, high operation speed, low power consumption, multilevel storage, and low cost,[11,12] thus they have the potential to replace the flash memory in the race of next-generation nonvolatile memory devices. It is often cited that the electrochemical redox process can induce the formation and annihilation of conducting filaments in the switching matrix,[11] giving rise to the RS phenomena. On the other hand, the electric-field-induced drift of oxygen vacancies and the impact ionization can cause changes in the Schottky barrier at the metal-insulator interface.[9] Other related models entailing the formation of phase-separated metallic domains and the Mott metal-insulator transition resulting from band bending were also proposed.[6,13]

As silicon is the foundation of traditional microelectronics, $SrTiO_3$ (STO) is the workhorse of the booming field of oxide electronics. The formation energy of oxygen vacancies is −4.8 eV in STO,[14,15] which is even lower than that in TiO_2 (−1.2 eV),[16] the canonical RS material.[17] Furthermore, STO is one of the most popular substrate for growing perovskite oxides, and the high quality single crystals are routinely available. In general, the physical properties of thin films often suffer from structural impurity and compositional inhomogeneity, which causes difficulties

[a]Author to whom correspondence should be addressed. Electronic mail: tao.wu@kaust.edu.sa

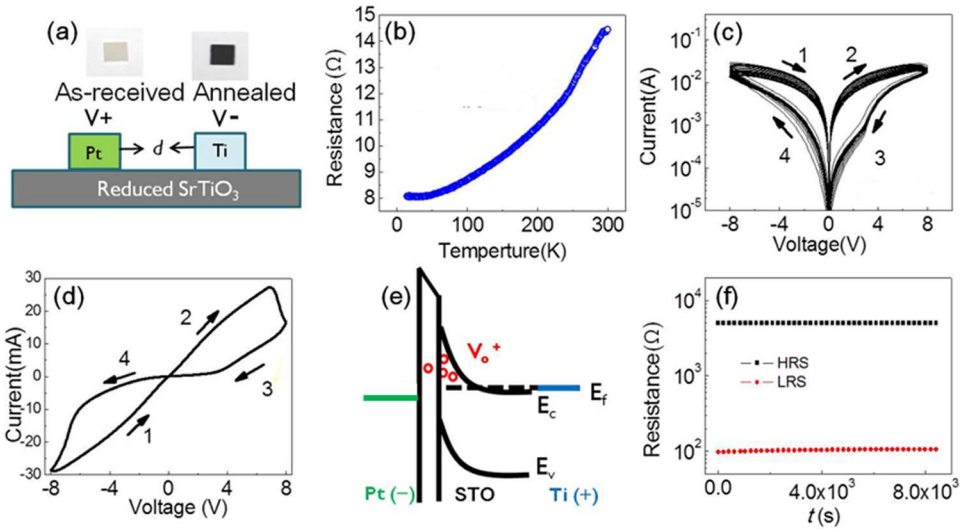

FIG. 1. (a) Schematic of the resistive switching device made of two in-plane metal electrodes separated by a distance *d* on a reduced STO substrate. In this Pt/STO/Ti junction, the anode and cathode are Pt and Ti, respectively. Also shown are the photos of the as-received and the vacuum-reduced STO substrates. (b) *R-T* curve of the reduced STO single crystal measured with a four-point configuration, showing the metal-like characteristics. (c) Semi-log plot of 30 consecutive *I-V* curves measured in a Pt/STO/Ti device, demonstrating the bipolar resistive switching. (d) Linear plot of a typical RS loop. (e) Schematic energy diagram of the Pt/STO/Ti junction. (f) Retention data of the device, and the ON/OFF ratio measured at 0.2 V is ∼50.

in elucidating the RS mechanisms in oxide devices. Thus, high quality STO single crystals can serve as a "pure" system to study the RS effect and elucidate the RS mechanisms. However, so far, STO has been received much less attention than other oxides in the RS research. In a pioneer study, Szot *et al.* showed that local modulation of the oxygen content and extended defects can lead to filament-based RS effect in thermally reduced STO single crystals.[8] In their study, Au or Pt conducting paste was used to paint electrodes with irregular shapes. In a later study, the same group made epitaxial STO films with a thickness of 500 nm on conducting Nb-doped STO substrates, and the top Pt electrodes were used to form active and switchable junctions with STO.[18] Reliable RS actions were also observed in polycrystalline oxygen-deficient STO thin films grown on Si substrates,[15,19] and in these reports Pt top electrodes were used. Very recently, ion milling was used to prepare high-density oxygen vacancies in STO, and bipolar RS behaviors were initiated by an Au-coated tip.[20] Furthermore, RS devices have also been constructed using STO thin films or single crystals doped with transition metals such as Cr, Nb, Co, and Mn, and the doping elements adjust the band structure of STO, making it electrically switchable.[21–24]

In the most-employed sandwich structures, the polycrystalline structure of oxide films sensitively depends on the synthesis details. It is often difficult to deposit high-quality single crystalline oxide films on top of conventional metal electrodes because the deposition process often requires high temperatures. In this study, we systematically investigate the effects of electrode engineering, in terms of both metal selection and shape modification, on the RS characteristics of planar devices made of self-doped STO single crystals. Our results suggest that the switching loop and the ON/OFF ratio can be tailored to a large extent by combining Ti and Pt as the electrode metals. The metal selection and the sweeping voltage are effective to tune the distribution of oxygen vacancies near the metal/STO interfaces and modulate the Schottky junctions at the Pt/STO interface, which in turn influences the RS characteristics. Furthermore, we studied and simulated the effect of different shapes of metal electrodes (rectangle, half circle, and triangle) in our RS experiments, which we found also play important roles in the device operations.

The schematic of our RS device is shown in Fig. 1(a). Here, we used a planar device configuration instead of the conventional vertical metal-oxide-metal capacitor-like structure. In our experiments, single crystalline (100)-oriented STO (one-side polished, 10 × 10 × 0.5 mm^3) substrates were

used. The as-received STO substrate is highly insulating and transparent (photo of the as-received substrate is shown in the inset of Fig. 1(a)). In order to introduce oxygen vacancies into STO, we annealed the single-crystal STO substrate in a vacuum of 10^{-7} mbar at 800 °C for 10 min. During this process, oxygen vacancies were created at the surface region of STO,[20] and consequently its resistance vs. temperature data show metal-like characteristics (Fig. 1(b)) because oxygen vacancies serve as singly ionized electron donors. As measured in a penetration experiment with ^{18}O tracer,[25] the diffusion constant of oxygen ions D along dislocations in STO is about 10^{-11} cm^2/s at 800 °C. Since the annealing time t is 10 min, the diffusion length $l = \sqrt{D \cdot t}$ of oxygen ions can be calculated to be about 0.8 μm, which can be taken as the thickness of the oxygen-vacancy-rich surface layer. Because of the generation of oxygen vacancies, the surface of STO substrate gains a black hue after reducing in vacuum. Ti and Pt electrodes with a typical dimension of 50 μm × 50 μm were sequentially defined on STO by lithography and lift-off, and the distance d between two electrodes (cathode and anode) was fixed at 3 μm.

The transport measurements were carried out in a probe station where a tough vacuum of 10^{-5} mbar is maintained. Unless specified otherwise, a forward bias applied to the device is defined as the current flowing from the Pt electrode into the STO.

As shown in the current vs. voltage (I-V) loops in Fig. 1(c), a typical bipolar RS behavior was observed in the Pt/STO/Ti device. In RS devices, electroforming is often used to prepare the switchable conducting filaments in the otherwise insulating matrix.[26] The elimination of the forming process in our devices simplifies the device operation and is an advantage compared to many devices reported in literature. As a result of oxygen reduction process, the pristine state of the device exhibits a low resistance of 200 Ω. As the voltage sweeps from −8 V, the device remains at the low resistance state (LRS); but at ∼7 V, it switches into the high resistance state (HRS), and the concurrent onset of negative differential resistance (NDR) can be clearly discerned in the linear plot of I-V loop in Fig. 1(d). Ruotolo and co-workers attributed the appearance of NDR to the avalanche injection in the space charge region.[27] Such NDR phenomena could also be related to the modification of conducting filaments under the application of a large electric field. The subsequence sweep of voltage from 8 V to −8 V switches the device back to the LRS. Figure 1(c) shows 30 I-V loops, and the set and reset processes are highly reliable.

In our device, the Ti electrode forms Ohmic contact with the switching STO, while the transport through the Pt/STO junction sensitively depends on the concentration of oxygen vacancies at the interface. The drift-diffusion motion of the oxygen vacancies and the associate mobility are dictated by both the electric field and the local temperature.[28] The initial negative bias on the Pt electrode attracts the positively charged oxygen vacancies toward the interface, which creates defect states in the depletion layer and reduces the Schottky barrier height and/or width,[29] resulting in the Ohmic transport and LRS (1 and 2 in Figs. 1(c) and 1(d)). On the other hand, the reverse process occurs when the voltage bias sweeps into the positive regime, and the oxygen vacancies are repelled from the Pt/STO interface, which restores the Schottky barrier and HRS (3 and 4 in Figs. 1(c) and 1(d)).

The energy band diagram corresponding to the LRS of Pt/STO/Ti junction is illustrated in Fig. 1(e). The work function of Ti (4.33 eV) is quite close to that of bulk STO (around 3.9 eV), and more importantly, the oxide formation free energy of Ti is among the lowest among all metals. Therefore, the Ti metal electrode serves as a reducing agent on the STO surface and forms an Ohmic contact at the Ti/STO interface. On the other hand, a Schottky barrier is established at Pt/STO interface. Our result suggests a scenario similar to what was proposed for TiO_2-based RS devices.[30] To test the stability of our planar STO device, we measured the data retention using a reading voltage of 0.2 V, and as shown in Fig. 1(f), both HRS and LRS can be retained for more than 3 h without any degradation, indicating good nonvolatile characteristics.

In order to shed light on the effect of metal selection in the RS operation, we fabricated and compared three devices with different combinations of metal electrodes, namely, Ti/STO/Pt, Pt/STO/Pt, and Ti/STO/Ti. As shown in Fig. 2(a), when the anode changes from Pt to Ti, the shape of the RS loop is reversed as compared to that in Fig. 2(a), i.e., the initial state of the device is HRS, and then the device switches to LRS as the voltage bias on the Ti electrode sweeps into the positive regime. In the Pt/STO/Pt device (Fig. 2(b)), Schottky barriers exist at both Pt/STO interfaces, and the ohmic behavior cannot be achieved in the RS loop because the oxygen vacancies are repelled

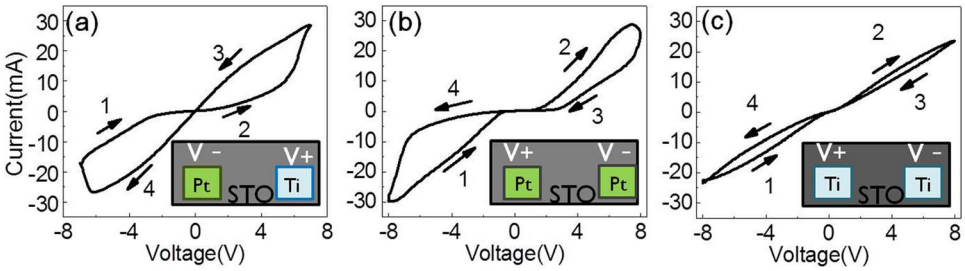

FIG. 2. (a) Dependence of the RS loop on the measurement configuration. Different from the device shown in Fig. 1(a), the anode and cathode here are Ti and Pt, respectively. (b) *I-V* characteristics of the Pt/STO/Pt device, and the ohmic-like characteristics of LRS is suppressed. (c) RS loop is much suppressed in the Ti/STO/Ti device as a result of the ohmic-like Ti/STO contacts.

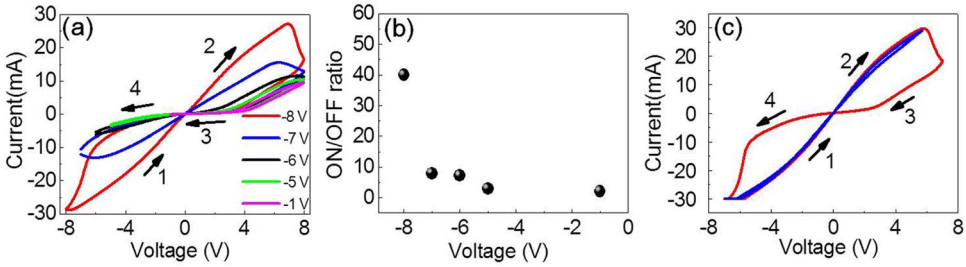

FIG. 3. (a) Dependence of the RS loop on the absolute value of the maximum negative voltage. Switching loop shrinks and NDR disappears if the absolute value of the magnitude of the maximum negative voltage is smaller than 6 V. (b) ON/OFF ratio vs. the maximum negative voltage. (c) Hysteresis of RS loop disappears if the voltage scan to the positive voltage regime is limited at 5.7 V (blue curve), which is before the onset of NDR occurs at 6 V. For comparison, a typical RS loop between −7 V and 7 V is also shown.

from one Pt/STO interface if they are attracted to the other one. The *I-V* loop in Fig. 2(b) suggests an almost symmetric profile of the oxygen vacancy distribution.[31] Finally, if both cathode and anode are Ti (Fig. 2(c)), the *I-V* loop appears much narrower because of the ohmic-like contact at the Ti/STO interface. Overall, these results suggest that RS mainly occurs at the Pt/STO interface, and selecting metal electrodes is effective in modulating the RS characteristics.

The Schottky barrier at the Pt/STO interface can be tailored by the lowest negative voltage bias applied to the Pt electrode because the positive charged oxygen vacancies which are pulled to the interface regime are responsible for preparing the LRS. We swept the bias voltage on Pt electrode as $-V_{max} \rightarrow +8\ V \rightarrow -V_{max}$, where the value of V_{max} was changed from 1 to 8 V. As demonstrated in Fig. 3(a), the switching hysteresis becomes less pronounced when the absolute value of the maximum negative voltage is smaller. Figure 3(b) plots the ON/OFF ratio measured at +0.5 V as a function of the maximum voltage, and it decreases from ∼40 to ∼2 as the lowest negative voltage changes from −8 V to −1 V.

Interestingly, the maximum positive voltage also exerts a significant influence on the RS behavior in the Pt/STO/Ti device. When we start the voltage sweep with a negative voltage of −7 V and limit the positive bias voltage to 5.7 V which is slightly smaller than the NDR onset voltage of ∼6 V, the RS loop disappears as demonstrated in Fig. 3(c). This phenomenon suggests that the appearance of NDR is critical for the development of RS. In the NDR regime, drift of oxygen vacancies and even local heating become more intense,[32,33] leading to the switching to the HRS. Under the influence of high positive voltage, oxygen vacancies are repelled away from the Pt/STO interface, which makes the Schottky barrier higher or wider, and it is clear that this process must be well controlled to realize reliable RS operation.

We hypothesize that electrode shape, like the shape corners in the lateral devices, may have some effects on the electric field distribution and the RS characteristics. In order to test this hypothesis, we prepared three different shapes of electrodes: rectangle, half circle, and triangle. As shown in

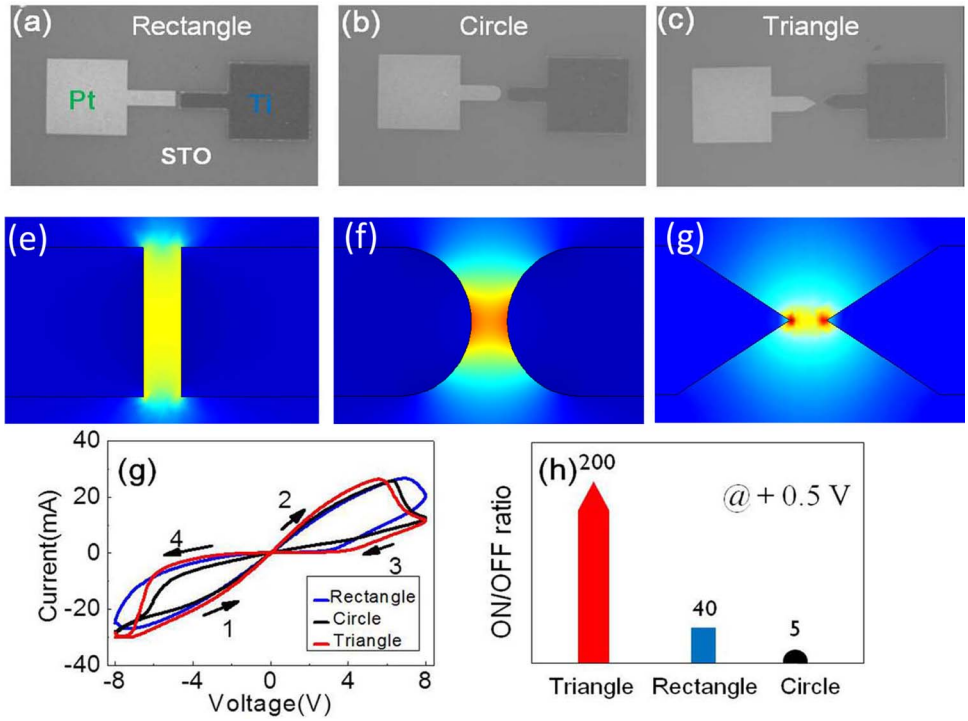

FIG. 4. SEM images of devices with (a) rectangle, (b) half-circle, and (c) triangle shaped electrodes. The finite-element simulation images of the intensity of electric field for (d) rectangular, (e) circular, and (f) triangular electrodes, respectively. (g) Corresponding *I-V* loops. In particular, triangle electrodes show a more pronounced switching loop compared to the circular and rectangular electrodes, and the ON/OFF ratios of the devices are shown in (h).

the scanning electron microcopy images in Figs. 4(a)–4(c), the distance between the electrodes is kept at 3 μm. To shed light on the effect of the electrode shape, we simulate the distribution of the electric field under a voltage bias of 0.5 V using the finite element method. The dielectric constant of STO is set as 300, and the distance between the electrodes is kept as 3 μm. As shown in Figs. 4(d)–4(f), the most intense electric field occurs at the geometric sharp corners of the electrodes, and the maximum electric field at a bias of 0.5 V is 1.733×10^5, 4.125×10^5, and 4.692×10^5 V/m for the circular, rectangular, and triangular electrodes, respectively. Therefore, the triangular electrode is most effective in producing intense electric field near the metal/oxide interface, facilitating the RS actions.

In previous experiments, the dependence of RS characteristics on the electrode material has been investigated,[34–36] but so far there has been no report on the effect of geometric shape of the electrodes. In our switching experiments, with the same operation parameters, RS can be observed in all three devices with different shapes. As shown in Fig. 4(g), a more pronounced resistive switching loop was observed in the device with triangular electrodes, and the corresponding ON/OFF ratio is ~200 at 0.5 V. The ON/OFF ratios are much lower in devices with rectangular and circular electrodes, and they are ~40 and 5, respectively (Fig. 4(h)). A low reading voltage of 0.5 V was consistently used to probe the ON/OFF resistance while avoiding the switching between different resistive states. The intense electric field at the triangular corners appears to be effective in causing the drift motion of charged oxygen vacancies and modifying the Schottky barrier at the Pt/STO interface. On the other hand, the smooth edge of the circular/rectangular electrodes cannot generate an electric field with very high local intensity, and the corresponding devices show a weaker performance.

Concurrent electronic and ionic transport phenomena in resistive switching devices challenge the current understanding of highly non-equilibrium processes in solids. Using transmission electron microscopy, we found that the Ti/STO interface is much abrupt than the Pt/STO interface.[37] In this work, we focus on the effects of electrode work function and geometry on the resistive switching

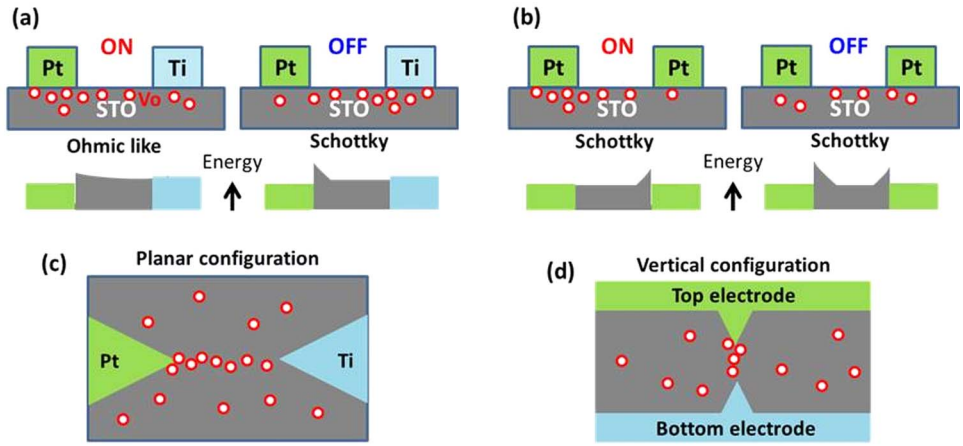

FIG. 5. (a) Schematic illustration of the relationship between the ON/OFF states of the Pt/STO/Ti device with the distribution of positively charged oxygen vacancies (upper figures). The lower figures illustrate the energy diagrams corresponding to the conversion between the Ohmic like and Schottky transport. (b) Illustration of the operating mechanism and energy diagrams of the Pt/STO/Pt device. Note that Schottky barriers exist in both ON and OFF states, but the polarity of rectification switches between the states. (c) Illustration of the planar RS device with triangular electrodes where the enhanced field near the tips guides the formation of conducting vacancy-rich filaments. (d) Conceptual illustration of potential vertical capacitor-type RS device with engineered electrode with sharp tips.

properties. We note here that the concept of Schottky or Ohmic contact should be applied only to the low voltage/current regimes of the *I-V* loops. Under high biases, tilting of band structures increases progressively, and mechanisms like charge injection and trap-assisted tunneling must be considered. This point can be confirmed by comparing the *I-V* data of the Pt/STO/Ti device shown in Figs. 1(d) and 2(a) with that of the Pt/STO/Pt device shown in Fig. 2(b). The main difference between the two devices exists in the low voltage/current region near origin: The ON/OFF states of the Pt/STO/Ti device correspond to switching between Schottky and Ohmic like transport, while Ohmic like behavior is never achieved in the Pt/STO/Pt device. As illustrated in Figs. 5(a) and 5(b), this different is rooted in the effect of drifting oxygen vacancies on the barrier characteristics, including both height and width, of the Pt/STO interface. There is a tradeoff in selecting electrode materials: The Pt/STO/Ti device generally presents higher ON/OFF ratios, while reading current is much lower in the Pt/STO/Pt device.

Under high voltage bias, scenario of Schottky barrier is no longer sufficient to describe the dynamic changes in transport properties of our devices. One critical aspect of the highly non-equilibrium process is the field-guided ionic motion of oxygen vacancies into forming conducting filaments (Fig. 5(c)). One may envisage that even the electrodes in the most-employed sandwich structure can be patterned with sharp features to control the formation and characteristic of conducting filaments. As illustrated in Fig. 5(d), the enhanced field near the tips of pyramids is expected to promote the filament formation and to reduce the operating voltage. Further investigation is needed to fabricate and characterize such electrode-engineered capacitor-type RS devices.

[1] R. Waser and M. Aono, Nature Mater. **6**, 833 (2007).
[2] D. B. Strukov, G. S. Snider, D. R. Stewart, and R. S. Williams, Nature (London) **453**, 80 (2008).
[3] F. Zhuge, S. S. Peng, C. L. He, X. J. Zhu, X. X. Chen, Y. W. Liu, and R. W. Li, Nanotechnology **22**, 275204 (2011).
[4] K. M. Kim, D. S. Jeong, and C. S. Hwang, Nanotechnology **22**, 254002 (2011).
[5] A. Beck, J. G. Bednorz, C. Gerber, C. Rossel, and D. Widmer, Appl. Phys. Lett. **77**, 139 (2000).
[6] M. J. Rozenberg, I. H. Inoue, and M. J. Sanchez, Phys. Rev. Lett. **92**, 178302 (2004).
[7] B. J. Choi *et al.*, J. Appl. Phys. **98**, 033715 (2005).
[8] K. Szot, W. Speier, G. Bihlmayer, and R. Waser, Nature Mater. **5**, 312 (2006).
[9] A. Sawa, Mater. Today **11**, 28 (2008).
[10] J. J. Yang, M. D. Pickett, X. M. Li, D. A. A. Ohlberg, D. R. Stewart, and R. S. Williams, Nat. Nanotechnol. **3**, 429 (2008).
[11] R. Waser, R. Dittmann, G. Staikov, and K. Szot, Adv. Mater. **21**, 2632 (2009).
[12] M. J. Lee *et al.*, Nature Mater. **10**, 625 (2011).
[13] T. Oka and N. Nagaosa, Phys. Rev. Lett. **95**, 266403 (2005).

[14] T. Tanaka, K. Matsunaga, Y. Ikuhara, and T. Yamamoto, Phys. Rev. B **68**, 205213 (2003).
[15] X. B. Yan, Y. D. Xia, H. N. Xu, X. Gao, H. T. Li, R. Li, J. Yin, and Z. G. Liu, Appl. Phys. Lett. **97**, 112101 (2010).
[16] J. B. Lu, K. S. Yang, H. Jin, Y. Dai, and B. B. Huang, J. Solid State Chem. **184**, 1148 (2011).
[17] K. Szot, M. Rogala, W. Speier, Z. Klusek, A. Besmehn, and R. Waser, Nanotechnology **22**, 254001 (2011).
[18] T. Menke, P. Meuffels, R. Dittmann, K. Szot, and R. Waser, J. Appl. Phys. **105**, 066104 (2009).
[19] D. H. Choi, D. Lee, H. Sim, M. Chang, and H. S. Hwang, Appl. Phys. Lett. **88**, 082904 (2006).
[20] H. Gross and S. Oh, Appl. Phys. Lett. **99**, 092105 (2011).
[21] W. F. Xiang, R. Dong, D. Lee, S. Oh, D. J. Seong, and H. Hwang, Appl. Phys. Lett. **90**, 052110 (2007).
[22] M. Janousch, G. I. Meijer, U. Staub, B. Delley, S. F. Karg, and B. P. Andreasson, Adv. Mater. **19**, 2232 (2007).
[23] X. T. Zhang, Q. X. Yu, Y. P. Yao, and X. G. Li, Appl. Phys. Lett. **97**, 222117 (2010).
[24] S. B. Lee *et al.*, Appl. Phys. Lett. **97**, 093505 (2010).
[25] K. Szot, W. Speier, R. Carius, U. Zastrow, and W. Beyer, Phys. Rev. Lett. **88**, 075508 (2002).
[26] D. S. Jeong, R. Thomas, R. S. Katiyar, J. F. Scott, H. Kohlstedt, A. Petraru, and C. S. Hwang, Rep. Prog. Phys. **75**, 076502 (2012).
[27] A. Ruotolo, C. W. Leung, C. Y. Lam, W. F. Cheng, K. H. Wong, and G. P. Pepe, Phys. Rev. B **77**, 233103 (2008).
[28] W. Jiang, M. Noman, Y. M. Lu, J. A. Bain, P. A. Salvador, and M. Skowronski, J. Appl. Phys. **110**, 034509 (2011).
[29] S. X. Wu, H. Y. Peng, and T. Wu, Appl. Phys. Lett. **98**, 093503 (2011).
[30] J. J. Yang, J. P. Strachan, F. Miao, M. X. Zhang, M. D. Pickett, W. Yi, D. A. A. Ohlberg, G. Medeiros-Ribeiro, and R. S. Williams, Appl. Phys. A: Mater. Sci. Process. **102**, 785 (2011).
[31] J. J. Yang, J. Borghetti, D. Murphy, D. R. Stewart, and R. S. Williams, Adv. Mater. **21**, 3754 (2009).
[32] A. S. Alexandrov, A. M. Bratkovsky, B. Bridle, S. E. Savel'ev, D. B. Strukov, and R. S. Williams, Appl. Phys. Lett. **99**, 202104 (2011).
[33] J. P. Strachan, D. B. Strukov, J. Borghetti, J. J. Yang, G. Medeiros-Ribeiro, and R. S. Williams, Nanotechnology **22**, 254015 (2011).
[34] S. Seo *et al.*, Appl. Phys. Lett. **87**, 263507 (2005).
[35] W. Y. Yang and S. W. Rhee, Appl. Phys. Lett. **91**, 232907 (2007).
[36] H. Y. Peng, G. P. Li, J. Y. Ye, Z. P. Wei, Z. Zhang, D. D. Wang, G. Z. Xing, and T. Wu, Appl. Phys. Lett. **96**, 192113 (2010).
[37] See supplementary material at http://dx.doi.org/10.1063/1.4827597 for STEM data.